The Journal of Chemical Physics

Memory effects in a random walk description of protein structure ensembles

Cite as: J. Chem. Phys. **150**, 064911 (2019); https://doi.org/10.1063/1.5054887
Submitted: 04 September 2018 . Accepted: 08 January 2019 . Published Online: 13 February 2019

Gerald R. Kneller, and Konrad Hinsen

The Journal of Chemical Physics ARTICLE scitation.org/journal/jcp

Memory effects in a random walk description of protein structure ensembles

Cite as: J. Chem. Phys. 150, 064911 (2019); doi: 10.1063/1.5054887
Submitted: 4 September 2018 • Accepted: 8 January 2019 •
Published Online: 13 February 2019

Gerald R. Kneller[1,2,3] and Konrad Hinsen[1,3]

AFFILIATIONS

[1]Centre de Biophysique Moléculaire, CNRS, Rue Charles Sadron, 45071 Orléans, France
[2]Université d'Orléans, Chateau de la Source-Av. du Parc Floral, 45067 Orléans, France
[3]Synchrotron Soleil, L'Orme des Merisiers, 91192 Gif-sur-Yvette, France

ABSTRACT

In this paper, we show that ensembles of well-structured and unstructured proteins can be distinguished by borrowing concepts from non-equilibrium statistical mechanics. For this purpose, we represent proteins by two different polymer models and interpret the resulting polymer configurations as random walks of a diffusing particle in space. The first model is the trace of the C_α-atoms along the protein main chain, and the second is their projections onto the protein axis. The resulting trajectories are subsequently analyzed using the theory of the generalized Langevin equation. Velocities are replaced by displacements relating consecutive points on the discrete protein axes and equilibrium ensemble averages by averages over appropriate protein structure ensembles. The resulting displacement autocorrelation functions resemble those of the velocity autocorrelation functions of simple liquids and display a minimum, which can be related to the lengths of secondary structure elements. This minimum is clearly more pronounced for well-structured proteins than for unstructured ones, and the corresponding memory function displays a slower decay, indicating a stronger "folding memory."

I. INTRODUCTION

The protein structure-function relationship is one of the basic concepts in structural biology, and it has, for several decades, driven the determination of protein structures by X-ray and neutron crystallography as well as by nuclear magnetic resonance (NMR) techniques. It was soon recognised that the protein function requires dynamic structures,[1–4] and one can observe a change in the paradigm over the last years, admitting that the protein function does not necessarily require well-defined structures. One speaks here of intrinsically disordered proteins (IDPs), where the term "disorder" describes the absence of well-defined secondary structure elements (SSEs) and may concern the whole protein or parts of it.[5–8] In contrast to well-structured proteins, for which more than 140 000 structures can be found at present in the Protein Data Bank (PDB),[9] much less is known about the possible conformations of IDPs. The main sources of information for IDP conformations are computer-generated models which are compatible with experimental data from structural NMR and small angle diffraction techniques. Corresponding databases are being built up[10,11] and becoming exploitable from a statistical point of view. One can therefore search for criteria that allow a distinction between structured and unstructured proteins on a purely statistical basis. Since protein structure databases contain structures and structure ensembles of *different* proteins, such statistical models should be based on the conformation of the protein main chain only. The simplest example is the polymer chain model by Kuhn,[12] which consists of equidistantly spaced point-like monomers and which can be transposed to proteins by associating each C_α-atom along the protein main chain with a monomer of the Kuhn chain. We note here that due to the rigid geometry of peptide bonds, the distances between consecutive C_α-atoms in proteins have an almost constant value of 0.4 nm. The polymer configurations in Kuhn's model are random chains, where all monomers are placed randomly at the fixed distance to their respective predecessor along the polymer chain. These freely jointed chains lead to a Gaussian model for the probability distribution of finding a monomer at a distance $\mathbf{r}$ from

a given monomer, and they can be interpreted as trajectories of Brownian particles whose subsequent positions in time correspond to the monomer positions along the polymer chain. The Markovian character of Brownian motion reflects the fact that the position of each monomer depends only on the position of its predecessor. The Gaussian chains thus have "zero folding memory." Kuhn's model was the motivation for the present work, where the concept of folding memory will be used in order to distinguish between ensembles of well-structured and (partially) unstructured proteins (IDPs).

II. PROTEINS AS DISCRETE PATHS

The standard discrete path representation of proteins is the C_α model, in which each residue is represented by its C_α-atom. In the following, we will also use a different path representation in which secondary structure elements (SSEs) are essentially filtered out. SSEs are characterised by a regular winding of the protein main chain with a typical period between 2 and 4 monomers (residues) and thus lead *a priori* to "trivial" folding memory effects on that scale. Using the ScrewFrame algorithm,[13] we obtain a description in which the helicoidal paths of SSEs are replaced by their axis. The global fold of a protein is described here as a succession of screw motions aligning successive discrete Frenet frames along the C_α-trace. The centres for the constructed screw motions then define a "polymer chain" along the protein axis. In contrast to the C_α-trace, where the distances between adjacent C_α-atoms are nearly constant, $\Delta \approx 0.38$ nm, the distances between adjacent screw motion centres vary and are considerably shorter. The constructed polymer chain may be associated with a Rouse chain, where the monomers are connected by springs.[14] The left part of Fig. 1 illustrates the construction of the screw motion centres (blue points) from a C_α-trace (red points) which has the form of an ideal helix such that the corresponding screw motion centres lie on a straight axis (except for the first and the last one). The two Frenet frames define the screw motion from "monomer" 2 to 3. For N C_α-atoms, there are N − 1 screw motion centres. The right part of the figure shows the corresponding analysis for myoglobin (PDB structure code 1AB6). It is important to note that ScrewFrame works for any C_α-trace, i.e., also for β-strands, which are "flat helices," and for unstructured parts of a protein. Secondary structure elements are characterised by recurrent screw motion parameters and in particular by a straight axis joining the screw motion centres. The ScrewFrame algorithm effectively leads to a tube model for proteins (indicated in transparent gray), where the local tube axis is defined by the succession of screw motion centres and the local radius by the radius of the respective screw motion. The tube can be considered as an excluded volume of the protein main chain. In polymer physics, tube models are used to explain the slow dynamics of reptation,[15,16] where the tube represents the space accessible to a single polymer inside the polymer matrix forming its environment, but the reptation model is obviously not a valid picture for the dynamics of protein main chains.

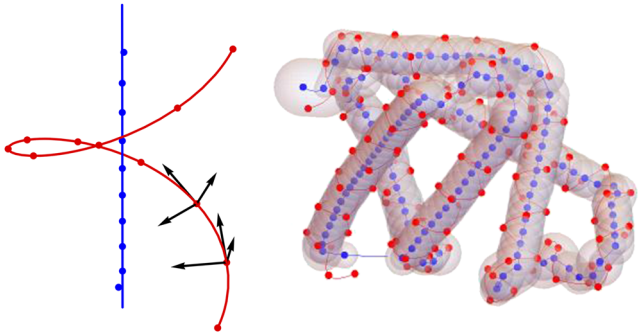

FIG. 1. Left: Exact helicoidal trace of C_α-atoms (red points) and corresponding screw motion centres (blue points). The figure also shows two consecutive Frenet frames, which are attached to C_α-atoms 2 and 3, respectively. Right: C_α-trace and corresponding screw motion centres for myoglobin (PDB structure code 1AB6). The local radius of the gray tube is defined by the radius of the corresponding screw motion.

III. DIFFUSIVITY OF PROTEIN PATHS

A. Mean square displacements

Starting from the analogy between polymer models and discrete stochastic paths, we first consider the ensemble-averaged mean square displacement (MSD),

$$W(n) = \left\langle \frac{1}{N_x - n} \sum_{k=0}^{N_x-1-n} (\mathbf{x}(k+n) - \mathbf{x}(k))^2 \right\rangle, \quad (1)$$

where N_x is the number of steps in the discrete path, $\mathbf{x}(k)$ ($k = 0, \ldots, N_x - 1$), and $n = 0, \ldots, P \ll N_x$ for statistical reasons. For our calculations, we used P = 100. The brackets in (1) denote an average over the protein structures in the given ensemble, where each protein structure counts equally. This weighting scheme is very different from thermal averaging of configurations in statistical mechanics, where each configuration is weighted with a Boltzmann factor, and corresponds to unconstrained maximum entropy weighting.[17] Equation (1) is constructed in complete analogy with time-dependent MSDs, as they are, for example, calculated from single particle tracking in biological systems or from molecular dynamics simulations. MSDs of discretely sampled trajectories are traced as a function of the time lag $n \equiv n\Delta t$, where Δt is the sampling step, whereas the MSDs presented in this paper are traced as a function of the dimensionless "residue lag." In this context, it may appear more appropriate to speak of "mean square distances" instead of "mean square displacements" because we are not considering moving particles. In order to keep the analogy with trajectory analyses, we keep, however, the first term in the following.

Figure 2 shows the MSD as a function of residue lag for well-structured and unstructured proteins. In the first case, we used protein structures from the ASTRAL database[18,19] and in the second from the pE-DB database.[10] The diffusion coefficients indicated in the plot have been obtained by fitting a linear expression of the form

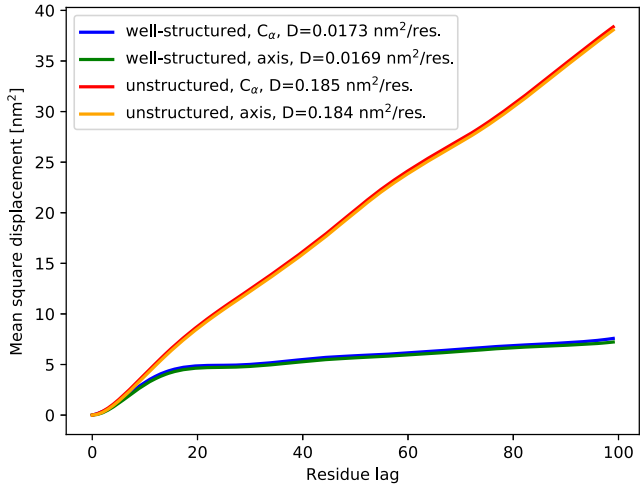

FIG. 2. Mean square displacement as a function of residue lag for well-structured and unstructured proteins. In both cases, the MSDs are shown for the C_α-traces and for the protein axes.

$$W(n) = 2Dn + a \tag{2}$$

to the MSD data for $n \geq 20$. This offset appears clearly in the data for well-structured proteins and corresponds roughly to the maximum length of protein secondary structure elements. Practically no differences can be found between the MSDs for the C_α-trace and the protein axis, but the diffusion coefficient for unstructured proteins is about ten times larger than that for well-structured proteins. We find $D \approx 0.18$ nm^2/res. in the first case and $D \approx 0.017$ nm^2/res. in the second. Using the polymer-trajectory analog, the asymptotic linear form of $W(n)$ for both well-structured and unstructured proteins corresponds to "normal diffusion." From this point of view, they behave as Gaussian chains or, equivalently, as trajectories of Brownian particles. As it will be shown in the following, the local behavior is, however, very different.

B. Displacement autocorrelation functions

In order to investigate the local properties of our two polymer models for well-structured and unstructured proteins, we make use of a well-known relation between the time-dependent MSD for a diffusing classical particle and its velocity autocorrelation function (VACF), $c_{vv}(\tau) = \langle \mathbf{v}(0)\cdot\mathbf{v}(\tau)\rangle$. Assuming the stationarity of the VACF, one derives[20]

$$W(t) = 2\int_0^t d\tau\,(t-\tau)c_{vv}(\tau), \tag{3}$$

where $\langle \ldots \rangle$ denotes a classical ensemble average over the phase space of the diffusing particle. The VACF itself fulfills an equation of motion of the form[21]

$$\dot{c}_{vv}(t) + \int_0^t d\tau\,\kappa_v(t-\tau)c_{vv}(\tau) = 0, \tag{4}$$

where the memory kernel $\kappa(t)_v$ can be formally expressed by the microscopic forces acting on the diffusing particle and between the solvent particles. In the following, only the general form of the equation of motion (4) is of importance. At the velocity level, the motion of a Brownian particle is described by the Langevin equation, $\dot{\mathbf{v}}(t) + \gamma\mathbf{v}(t) = \mathbf{f}_s(t)$, where $\mathbf{f}_s(t)$ is the white noise and $\gamma > 0$ is the friction constant. The memory kernel has the form $\kappa_v(t) = \gamma\delta(t)$, where $\delta(t)$ is the Dirac delta function. Brownian motion is thus "memory-less," and the VACF has the form $c_{vv}(t) = \langle|\mathbf{v}|^2\rangle \exp(-\gamma t)$. We will now investigate which kind of VACF and corresponding memory function will emerge from the polymer paths representing well-structured and unstructured proteins. Here the VACF becomes, in fact, a discrete displacement autocorrelation function (DACF),

$$c_{dd}(n) = \left\langle \frac{1}{N_d - n}\sum_{k=0}^{N_d-1-n} \mathbf{d}(k+n)\cdot\mathbf{d}(k)\right\rangle, \tag{5}$$

where $\mathbf{d}(k) = \mathbf{x}(k+1) - \mathbf{x}(k)$ $(k = 0, \ldots, N_d - 1)$ and $N_d = N_x - 1$. Using that the convolution is commutative, the memory function equation (4) is replaced by the discrete version

$$\Delta c_{dd}(n) + \sum_{k=0}^{P} w(k)c_{dd}(n-k)\kappa_d(k) = 0, \tag{6}$$

for $n = 0, \ldots, P \ll N_d$. Here $w(k)$ are integration weights according to the second order (trapezoidal) rule for numerical integration, $w(0) = w(P) = 1/2$ and $w(k) = 1$ for $k = 2, P-1$, and Δ denotes a numerical derivative of the second order. Equation (6) represents a triangular linear system of equations for $\kappa_d(k)$ $(k = 0, \ldots, P)$, which can be recursively solved. The second order approximation for numerical integration and differentiation assures that, to a good approximation, $\kappa_d(n) \propto \lambda\delta_{0n}$ if $c_{dd}(n) = c_{dd}(0)\exp(-\lambda n)$ and $N_d \gtrsim 100$.

Figure 3 shows the DACFs for well-structured (upper panel) and unstructured proteins (lower panel). In contrast

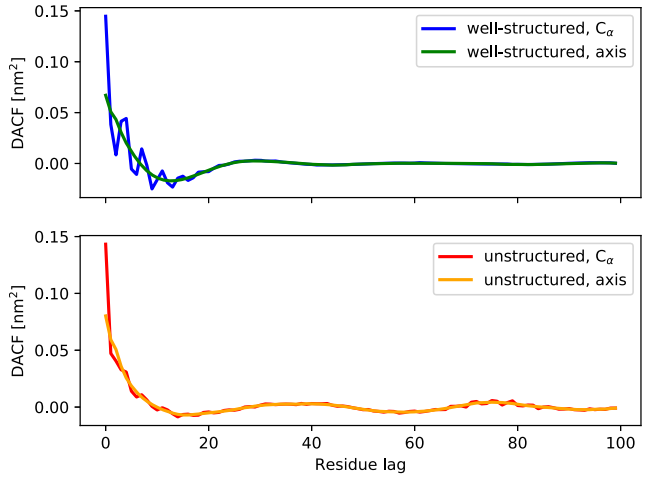

FIG. 3. Upper panel: DACFs for well-structured proteins comparing the C_α-traces and protein axes. Lower panel: The same for unstructured proteins.

to the MSDs, there is a clear difference between the DACFs corresponding, respectively, to the C_α-trace and the protein axis. The DACFs in the latter case are clearly smoother and do not present the fast oscillations at the beginning which are visible in the DACFs for the C_α-traces which are particularly pronounced for well-structured proteins. They can be attributed to secondary structure elements, where the direction of the displacements changes periodically with residue lags of approximately 2 (β-strands) to 4 (α-helices). The DACF for the protein axis of well-structured proteins has a striking similarity with the VACF of simple liquids. A surprising result of Rahman's historic simulation of liquid argon[22] was that the VACF for such a system does not decay exponentially, as for the Langevin model, but displays damped oscillations which are ascribed to rattling motions of the diffusing molecules in the case of nearest neighbours. Here the lag time corresponding to the first minimum corresponds to the typical time for a reversal of its velocity. In analogy, the DACF for the protein axis of well-structured proteins displays a pronounced minimum for residue lags of about $n = 18$, which means that the displacement vector **d** tends to invert its direction after 18 consecutive steps. Knowing that typical secondary structure elements have about this length, such a behaviour could be explained by the typical "helix-loop-helix" successions in well-structured proteins like myoglobin. Here the term "helix" must be understood in the sense of the ScrewFrame algorithm, i.e., as a regular secondary structure element which includes α-helices and β-strands. To investigate this point in more detail, we have computed the DACFs for the protein axis of well-structured proteins separately for sub-ensembles of protein structures containing, respectively, essentially α-helices and β-strands and recording in both cases histograms for the lengths of these secondary structure elements. Figure 4 shows clearly that the first minima of the axis DACFs are correlated with the maximum lengths of the secondary

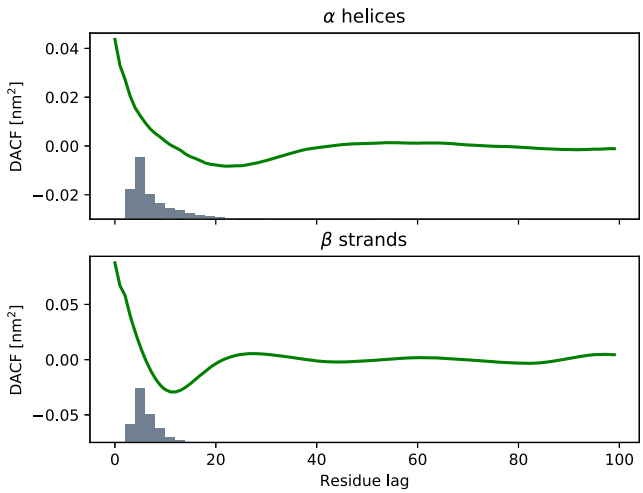

FIG. 4. Upper panel: DACFs for the protein axis of well-structured proteins containing essentially α-helices and histogram for the lengths of the latter. Lower panel: The same for β-strands.

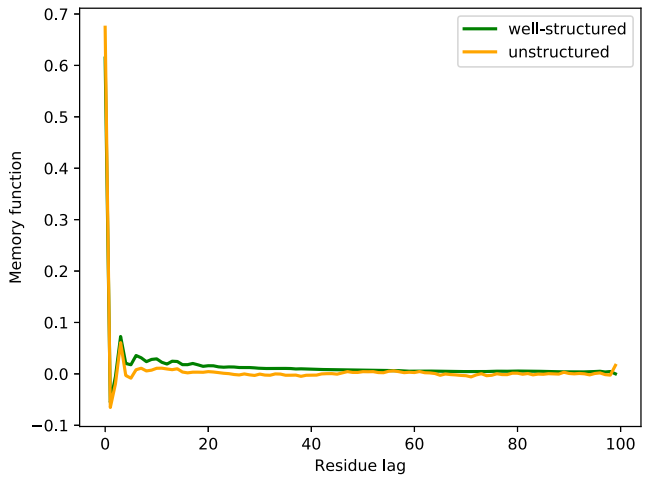

FIG. 5. Memory kernel of the protein axis DACF for well-structured proteins and unstructured proteins.

structure elements, which confirms the hypothesis that the first minimum of the DACF reflects effectively the recurrent "helix-loop-helix" motif in globular well-structured proteins. This motif and its presence in unstructured proteins should also be reflected in the corresponding memory kernels of the DACF. Figure 5 shows the memory kernels for protein axis DACFs of well-structured proteins and unstructured proteins. Although the difference is small, it is systematic: The memory function corresponding to the DACF of well-structured proteins is systematically larger than its counterpart for unstructured proteins, indicating stronger "folding memory." The slight oscillations in the latter case should not be overinterpreted since they might be artefacts due to insufficient statistics.

IV. CONCLUSIONS

Our study shows that suitably defined polymer models for proteins enable a meaningful statistical analysis of their folding properties on the basis of "polymer paths." Here each path is a succession of points that represent the residues, and two types of paths are considered: (1) the C_α-representation, where each residue is represented by its C_α-atom, and (2) the ScrewFrame representation, where each residue is represented by a projection of the C_α position onto an appropriately constructed protein main axis. The resulting paths are analyzed within a theoretical framework that is inspired by the theory of the generalized Langevin equation. We show, in particular, that the memory functions associated with the displacement autocorrelation function along the protein chain display effects of "folding memory" for well-structured proteins, as compared to IDPs. Although the statistical basis for unstructured proteins is still fairly small, the theoretical framework allows for discriminating between ensembles of well-structured and unstructured proteins. The next step will be to develop suitable simple memory function models which explain the

data at least semi-quantitatively and which have a physical interpretation.

SUPPLEMENTARY MATERIAL

The complete source code of our analysis software and the input datasets are available as supplementary material to this article.

REFERENCES

[1]R. H. Austin, K. W. Beeson, L. Eisenstein, H. Frauenfelder, and I. C. Gunsalus, Biochemistry **14**, 5355 (1975).
[2]N. Alberding, R. H. Austin, S. S. Chan, L. Eisenstein, H. Frauenfelder, I. C. Gunsalus, and T. M. Nordlund, J. Chem. Phys. **65**, 4701 (1976).
[3]H. Hartmann, F. Parak, W. Steigemann, G. Petsko, D. Ponzi, and H. Frauenfelder, Proc. Natl. Acad. Sci. U. S. A. **79**, 4967 (1982).
[4]H. Frauenfelder, S. G. Sligar, and P. G. Wolynes, Science **254**, 1598 (1991).
[5]H. J. Dyson and P. E. Wright, Nat. Rev. Mol. Cell Biol. **6**, 197 (2005).
[6]R. B. Best, Curr. Opin. Struct. Biol. **42**, 147 (2017).
[7]A. Soranno, A. Holla, F. Dingfelder, D. Nettels, D. E. Makarov, and B. Schuler, Proc. Natl. Acad. Sci. U. S. A. **114**, E1833 (2017).
[8]P. Kulkarni and V. N. Uversky, PROTEOMICS **18**, 1800061 (2018).
[9]P. W. Rose, A. Prlić, C. Bi, W. F. Bluhm, C. H. Christie, S. Dutta, R. K. Green, D. S. Goodsell, J. D. Westbrook, J. Woo *et al.*, Nucleic Acids Res. **43**, D345 (2015).
[10]M. Varadi, S. Kosol, P. Lebrun, E. Valentini, M. Blackledge, A. K. Dunker, I. C. Felli, J. D. Forman-Kay, R. W. Kriwacki, R. Pierattelli *et al.*, Nucleic Acids Res. **42**, D326 (2014).
[11]M. Necci, D. Piovesan, Z. Dosztányi, P. Tompa, and S. C. E. Tosatto, Bioinformatics **34**, 445 (2018).
[12]W. Kuhn, Kolloid-Z. **68**, 2 (1934).
[13]G. R. Kneller and K. Hinsen, Acta Crystallogr. D **71**, 1411 (2015).
[14]P. E. Rouse, J. Chem. Phys. **21**, 1272 (1953).
[15]P. G. de Gennes, J. Chem. Phys. **55**, 572 (1971).
[16]T. C. B. McLeish, Adv. Phys. **51**, 1379 (2002).
[17]A. Papoulis, *Probablity, Random Variables, and Stochastic Processes*, 3rd ed. (McGraw-Hill, New York, 1991).
[18]J.-M. Chandonia, G. Hon, N. S. Walker, L. Lo Conte, P. Koehl, M. Levitt, and S. E. Brenner, Nucleic Acids Res. **32**, D189 (2004).
[19]N. K. Fox, S. E. Brenner, and J. M. Chandonia, Nucleic Acids Res. **42**, D304 (2013).
[20]J. Boon and S. Yip, *Molecular Hydrodynamics* (McGraw-Hill, New York, 1980).
[21]R. Zwanzig, *Nonequilibrium Statistical Mechanics* (Oxford University Press, 2001).
[22]A. Rahman, Phys. Rev. **136**, A405 (1964).